# Mobility of a semiflexible chain confined in a nanochannel

Douglas R. Tree,[1] Yanwei Wang,[2] and Kevin D. Dorfman[1,*]

[1] *Department of Chemical Engineering and Materials Science, University of Minnesota — Twin Cities, 421 Washington Ave. SE, Minneapolis, MN 55455*

[2] *Jiangsu Key Laboratory of Advanced Functional Polymer Design and Application, Department of Polymer Science and Engineering, College of Chemistry, Chemical Engineering and Materials Science, Soochow University, 199 Ren-ai Road, Suzhou, 215123, P.R. China*

(Dated: March 2, 2012)

## Abstract

The classic results of de Gennes and Odijk describe the mobility of a semiflexible chain confined in a nanochannel only in the limits of very weak and very strong confinement, respectively. In moderate confinement, the chain mobility exhibits a broad plateau as a function of extension before transitioning to an Odijk regime. For DNA in a high ionic strength buffer, this Rouse-like behavior persists over most of the measurable chain extensions seen in experiments. In contrast, flexible chains are described by the classical theories throughout the full range of extension.

PACS numbers: 87.15.ak, 87.15.hj, 87.14.gk

The configurations and dynamics of a flexible chain confined in a tube were described quite some time ago by de Gennes [1–3] and Odijk [4]. Emerging genomics technologies such as DNA barcoding [5, 6] have brought to the forefront the comparable problem of describing semiflexible chains when they are confined in a nanochannel [7, 8]. In this Letter, we show that the classical results for the de Gennes and Odijk regimes, which describe the dynamics of flexible chains over the full range of confinement, are the limiting cases for semiflexible chains such as DNA. As a result, these theories cannot describe data on the dynamics of semiflexible chains over the experimentally relevant range of chain extensions ($\sim 20\%$ to $\sim 80\%$). We have developed a description of the mobility of a semiflexible chain confined in a nanochannel that highlights the stark differences between the dynamics of flexible and semiflexible chains. In particular, we show that the common assumption that the friction coefficient of a confined, semiflexible chain is proportional to its extension is incorrect.

Let us first define what we mean by a semiflexible chain, since this term changes in different contexts [9]. The polymer is described by its contour length $L$, persistence length $l_p$, and effective width $w$, such that the chain consists of $N = L/l_p$ persistence lengths. Often, the term "semiflexible" is used in a global context to describe a chain where $L \approx l_p$, corresponding to a semiflexible filament such as actin. In our study of chains confined in nanochannels, we are concerned with the local flexibility of the chain on the length scale of the channel size, $D \approx l_p$. In this context the anisotropy of the "monomers" matters, with a flexible chain corresponding to $l_p/w \approx 1$ and a semiflexible chain corresponding to $l_p/w \gg 1$ [10].

In particular, we will focus on double-stranded DNA in a high ionic strength buffer that screens electrostatic interactions, which has frequently been used as a model system for a confined polymer [11]. In these conditions, DNA is clearly a semiflexible chain, with $l_p = 53$ nm [12] and $w = 4.6$ nm [13]. As we will see, this high degree of anisotropy limits the applicability of the classic results from de Gennes [1–3] to very small values of the fractional extension. The DNA used in experiments can be quite long, normally tens of microns in length. As a result, the chain is flexible in the global sense since $L \gg l_p$.

We already know that the semiflexible nature of DNA strongly affects its equilibrium extension [13–16]. Figure 1 shows how the average chain extension, $\langle X \rangle$, depends on the degree of confinement for a flexible chain and semiflexible chain. These data were generated by modeling the chain as a series of $N_b = 2048$ touching beads [17] of size $w$ that interact

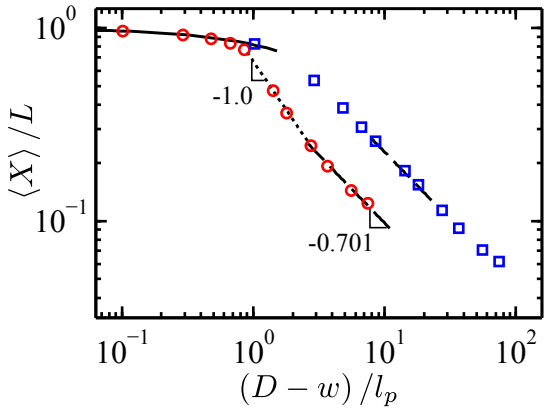


FIG. 1. (color online) Averaged extension of a flexible ($l_p = 5.3$nm, blue squares) and a semiflexible ($l_p = 53$nm, red circles) chain containing 2048 touching beads of width $w = 4.6$ nm as a function of the effective channel width, $D - w$, available to the chain. To aid the eye, lines corresponding to the Odijk regime (solid), transition regime (dotted), and extended de Gennes/de Gennes regimes (long dashed) are shown.

by a hardcore excluded volume interactions. To give the chain a persistence length of $l_p$, a bending potential is enforced between trios of beads according to the discrete wormlike chain model [16, 18]. Analogous to our prior work [16], we generated an equilibrium ensemble of chain configurations using Monte Carlo simulations with reptation, crankshaft and pivot moves [19]. The simulation was run in each case until the statistical errors, corrected for the time series autocorrelation [20], were smaller than the size of the plot symbols.

The classical theories [1, 2, 4] provide a complete description for the extension of the flexible chain. Over almost the full range of extension, the flexible chain is in the de Gennes regime [1, 2]. Here, the chain consists of isometric compression blobs of characteristic volume $D^3$ containing a subchain of length $L_{\rm sub} \cong D^{5/3}(wl_p)^{-1/3}$ [14]. The corresponding extension is $\langle X \rangle \cong L(wl_p)^{1/3}D^{-2/3}$. A more precise calculation yields $\langle X \rangle \sim D^{(\nu-1)/\nu}$ with $\nu = 0.5877$ being the Flory parameter [16]. In the tightest channels, the chain crosses over into the Odijk regime [4], where the chain consists of a series of deflection segments. The extension here is $\langle X \rangle = L[1 - 2\alpha\,(D/l_p)^{2/3}]$ with $\alpha = 0.09137$ a universal prefactor [21].

In contrast, the classical theories [1, 2, 4] only correspond to the limiting cases for the extension of a semiflexible chain. Indeed, in order for a semiflexble chain to be able to reach a de Gennes regime, the polymer must have a length of at least $L \cong {l_p}^3/w^2$ in a

channel that is larger than $D \cong {l_p}^2/w$ [14, 16]. As a semiflexible chain is compressed by decreasing the channel size, the blobs become anisometric [13, 14, 16] with size $D^2H$, where $H \cong (Dl_p)^{2/3}w^{-1/3}$. Each one of these cylindrical blobs contains a subchain of length $L_* \cong {l_p}^{1/3}D^{4/3}w^{-2/3}$. This regime was named the "extended" de Gennes regime [16] because the scaling for the extension in the de Gennes regime, $\langle X \rangle \cong L(wl_p)^{1/3}D^{-2/3}$, extends to the case of anisometric compression blobs. When the channel size approaches the order of the persistence length, $D \approx l_p$, and the chain can no longer form blobs. Here the behavior crosses into a transition regime where several simulations [15, 16], including our results in Fig. 1, indicate that the extension scales like $\langle X \rangle \sim D^{-1}$ [15, 16]. The free energy of these configurations is unknown, and it is not clear yet if the behavior is universal. Finally, when $D \ll l_p$, the other classical limit of Odijk is recovered, as in the case of flexible chains.

As the anisotropy of the monomers increases, the importance of the transition regime becomes increasingly important; the maximum extension in the extended de Gennes regime is $\langle X \rangle / L \cong (w/l_p)^{1/3}$. When DNA in a high ionic strength buffer is used as a model confined polymer [7, 8], the extended de Gennes regime and, in particular, the transition regime encompass almost the entire experimental range of extensions [16]. Indeed, the existence of these additional regimes explains [16] the disagreement between early experiments on DNA extension in nanochannels [8] and the de Gennes model.

Let us now consider the mobility of a confined semiflexible chain. By applying an infinitesimal force $f_x$ that is uniformly distributed along the chain, the corresponding velocity along the channel axis is

$$v_x = \mu f_x = \langle \Omega_{xx} \rangle f_x \tag{1}$$

where $\mu$ is the mobility of the chain. As seen in eq. (1), we can obtain the Kirkwood approximation to the mobility [22, 23] from the appropriate component of the hydrodynamic tensor, $\Omega_{xx}$, where the brackets refer to an average over the equilibrium distribution of chain configurations.

According to the blob theory [2, 3], the mobility in the extended de Gennes regime should be the same as the de Gennes regime, even though the blobs are now anisometric. To see why, we simplify eq. (1) for the Kirkwood chain mobility in terms of the pair-correlation function, $g(r)$, following de Gennes [2],

$$\mu = N^{-1} \int g(r)\Omega(r) d^3\mathbf{r} \tag{2}$$

In the blob theory [3] the pair-correlation function is replaced with $c$, the number concentration of segments inside a blob, and the hydrodynamic screening by the walls is approximated by $\Omega(r) = 1/\eta r$ for $r < D$ and exponentially decaying for $r > D$ [2, 3], where $\eta$ is the solvent viscosity. Since we only need an approximate result, the remainder of the calculation is simplified by using spherical coordinates and integrating over the solid angle [2],

$$\mu = \frac{4\pi c}{N} \int_0^D \frac{1}{\eta r} r^2 dr \approx \frac{cD^2}{\eta N} \tag{3}$$

In the de Gennes regime, the monomer concentration in the blobs is $c \cong (L_{\mathrm{sub}}/l_p)/D^3$, which yields $c \cong w^{-1/3} l_p^{-4/3} D^{-4/3}$. Recalling that $N = L/l_p$, we recover the classic result that the friction scales with chain extension [3]

$$\mu \sim (1/\eta L) \langle X/L \rangle^{-1} \tag{4}$$

In the extended de Gennes regime, the density of segments is $(L_*/l_p)/(D^2 H)$, which again yields $c \cong w^{-1/3} l_p^{-4/3} D^{-4/3}$. As a result, the blob theory predicts the diffusion in the extended de Gennes regime is given by eq. (4). Since the blob theory breaks down in the transition regime [16], the logic leading to eq. (4) is no longer valid.

We computed the Kirkwood mobility through a Monte Carlo integration of eq. (1) [24]. For a given chain configuration, we computed the $3 \times 3$ chain hydrodynamic tensor

$$\mathbf{\Omega} = \frac{1}{{N_b}^2} \sum_{i,j}^{N_b} \left[ \frac{\delta_{ij}}{6\pi\eta a} \mathbf{I} + (1 - \delta_{ij}) \mathbf{\Omega}^{\mathrm{OB}}(\mathbf{r}_{ij}) + \mathbf{\Omega}^{\mathrm{W}}(\mathbf{r}_i, \mathbf{r}_j) \right] \tag{5}$$

In the latter, $\delta_{ij}$ is the Kronecker delta, $\mathbf{r}_i$ and $\mathbf{r}_j$ are the positions of bead $i$ and $j$ respectively and $\mathbf{r}_{ij} = \mathbf{r}_j - \mathbf{r}_i$. The hydrodynamic tensor also introduces the bead hydrodynamic radius, $a$, which is often conflated with the effective width, despite the fact that they arise from quite different phenomena. We chose $a = 1.38$ nm so that the chain mobilities in free solution for $l_p = 53$ nm matched experimental values for DNA [25].

The hydrodynamic tensor includes a self-diffusion term, a free-solution Oseen-Burgers tensor [26], $\mathbf{\Omega}^{\mathrm{OB}}$, and a wall term, $\mathbf{\Omega}^{\mathrm{W}}$, due to the effects of the no-slip condition at the channel boundaries. The Oseen-Burgers tensor is acceptable in this calculation because the beads are hard spheres, and do not suffer from unphysical behavior caused by bead-bead overlap. The wall term was calculated using a numerical solution of Stokes equation, similar to Jendrejack *et al.* [26]. We employed a second-order finite difference approach with

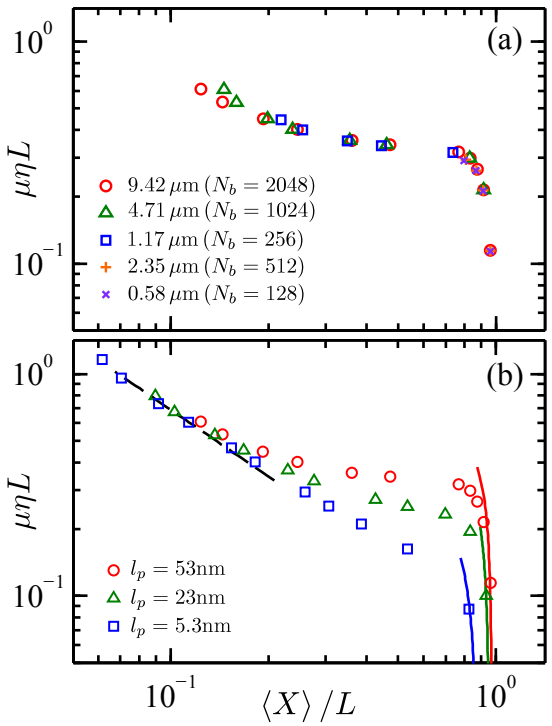


FIG. 2. (color online) Mobility versus extension. All simulations correspond to $w = 4.6$ nm and $a = 1.38$ nm. (a) Results for five different chain lengths for $l_p = 53$ nm. (b) Results for three different persistence lengths for $L = 9.42$ $\mu$m ($N_b = 2048$ beads). The dashed line is the scaling of eq. (4). At large extensions, each chain approaches the Odijk regime (solid lines), where the mobility is a function of $l_p$ [27].

a staggered, three-dimensional, uniform, Carteisan mesh and mass-conserving boundary conditions. Due to the prohibitive computational time needed to solve the hydrodynamic problem for each chain configuration, the wall term was calculated and stored on a grid, and subsequently linearly interpolated during Monte Carlo averaging. Finally, we note that in each case the statistical error of the computed diffusivity, corrected for the time series autocorrelation [20], are smaller than the size of all plot symbols.

Figure 2a shows the results for the mobility of a semiflexible chain as a function of its extension. In the largest channels, corresponding to the smallest fractional extensions, the channel provides minimal confinement and the chains are approaching the Zimm free solution mobility, $\mu \sim L^{-3/5}$. Outside of this limit, the friction due to the walls is substantial. If we neglect the wall term in eq. (5) for a channel size of 80 nm, the resultant mobility is more than 5 times larger. However, there is a broad plateau in the mobility as a function of the

channel diameter.

In Fig. 2b, we compare the mobility as a function of extension for different persistence length chains. Equation (4) is a reasonable description for the flexible chain with $l_p = 5.3$ nm all the way to the transition to the Odijk regime. Fitting the data gives $\mu \sim \langle X \rangle^{-0.874}$ ($R^2 = 0.998$) which agrees very well with the value of $\mu \sim \langle X \rangle^{-0.61/0.7015}$ obtained from other flexible chain calculations [26, 28]. However, the scaling in eq. (4) is qualitatively incorrect for the semiflexible chain with $l_p = 53$ nm over almost the full range of extension. We also simulated an intermediate persistence length $l_p = 23$ nm and found an intermediate result; for short extension this chain obeys de Gennes scaling but it still exhibits a broad transition towards the Odijk result.

The key to understanding the difference between the results for flexible and semiflexible chains lies in their draining behavior, which has also been observed for DNA in slits [29]. In the classical de Gennes regime, the blobs can be thought of as free-solution coils on length scales smaller than the channel size, and are clearly non-draining [2]. At the other classical limit, the Odijk regime, the mobility can be approximated as a slender rod where the interactions are screened on the order of $D$ [8, 27]. There must clearly be some crossover between the behavior of non-draining blobs in the weakly confined limit to the freely-draining chain in the strongly confined limit. In the case of flexible chains, this crossover is short, as was seen with the extension behavior. If the confinement does not force a rod-like conformation, the chains can only form blobs and quickly become non-draining.

In the semiflexible case, the intermediate regimes that arise as the channel size increased due to the large monomer anisotropy delay the crossover from rod-like behavior to blob behavior (for the conformation) and thus extend the crossover from free-draining to non-draining behavior (for the mobility). The transition and extended de Gennes regimes therefore give rise to the mobility plateau, because they force the chain to persist in elongated states such that the chain remains Rouse-like for larger channel sizes. The fact that these regimes give rise to the mobility plateau can be seen from the correspondence between the fractional extensions for the mobility plateau limits and the regime limits. To illustrate this, consider the extension of a chain with a persistence length of 23 nm. In this case the de Gennes regime ends at a fractional extension of about 0.2, and the Odijk regime begins at a fractional extension of about 0.7. For $l_p = 53$ nm, the semiflexible regimes begin and end at fractional extensions of 0.15 and 0.8 respectively. These extensions closely align with the

extensions in Fig. (2)b that correspond to the beginning and ending of the mobility plateau. Thus the intermediate regimes can explain both the existence of the mobility plateau and the fact that it grows with increasing persistence length.

While we have focused exclusively on the dynamics of DNA in a high ionic strength buffer, where electrostatic interactions are screened, there are DNA barcoding devices [5] that use high ionic strengths to stiffen the DNA backbone. As the ionic strength decreases, the predicted values for the effective width and persistence length begin to converge [30]. Our analysis thus predicts that DNA will obey the de Gennes prediction in eq. (4) in a sufficiently low ionic strength such that $l_p/w \approx 1$ and a large enough channel such that this very high persistence length chain can form compression blobs. These experiments are technically challenging, since the length of DNA required to reach the de Gennes regime in a low ionic strength buffer is enormous.

In this Letter, we have clearly shown that the hydrodynamics of confined semiflexible chains deviate significantly from the classic prediction for a flexible chain in eq. (4) [2, 3]. As there are a large number of publications using DNA in a high ionic strength buffer as a model polymer, it is important to keep in mind the stark differences between the dynamics of semiflexible chain such as DNA and the more flexible chains often encountered in polymer physics [11].

We acknowledge useful discussions with Prof. D.C. Morse. This work was supported by the NIH (R01-HG005216) and was carried out in part using computing resources at the University of Minnesota Supercomputing Institute.

---

* dorfman@umn.edu

[1] M. Daoud and P.-G. de Gennes, J. Phys. (Paris) **38**, 85 (1977).

[2] P.-G. de Gennes, *Scaling Concepts in Polymer Physics* (Cornell University Press, Ithaca, NY, 1979).

[3] F. Brochard and P.-G. de Gennes, J. Chem. Phys. **67**, 52 (1977).

[4] T. Odijk, Macromolecules **16**, 1340 (1983).

[5] K. Jo, D. M. Dhingra, T. Odijk, J. J. de Pablo, M. D. Graham, R. Runnheim, D. Forrest, and D. C. Schwartz, Proc. Natl. Acad. Sci. USA **104**, 2673 (2007); Y. Kim, K. S. Kim, K. L.

Kounovsky, R. Chang, G. Y. Jung, J. J. de Pablo, K. Jo, and D. C. Schwartz, Lab Chip **11**, 1721 (2011).

[6] S. K. Das, M. D. Austin, M. C. Akana, P. Deshpande, H. Cao, and M. Xiao, Nucleic Acids Res. **38**, e177 (2010); S. F. Lim, A. Karpusenko, J. J. Sakon, J. A. Hook, T. A. Lamar, and R. Riehn, Biomicrofluidics **5**, 034106 (2011).

[7] J. O. Tegenfeldt, C. Prinz, H. Cao, S. Chou, W. W. Reisner, R. Riehn, Y. M. Wang, E. C. Cox, J. C. Sturm, P. Silberzan, and R. H. Austin, Proc. Natl. Acad. Sci. USA **101**, 10979 (2004).

[8] W. Reisner, K. J. Morton, R. Riehn, Y. M. Wang, Z. Yu, M. Rosen, J. C. Sturm, S. Y. Chou, E. Frey, and R. H. Austin, Phys. Rev. Lett. **94**, 196101 (2005).

[9] F. Wagner, G. Lattanzi, and E. Frey, Phys. Rev. E **75**, 050902(R) (2007).

[10] A. Yu. Grosberg and A. R. Khokhlov, *Statistical Physics of Macromolecules* (American Institute of Physics, 1994) pp. 90–92; M. Rubinstein and R. Colby, *Polymer Physics* (Oxford University Press, 2003) pp. 98–102.

[11] F. Latinwo and C. M. Schroeder, Soft Matter **7**, 7907 (2011).

[12] C. Bustamante, J. F. Marko, E. D. Siggia, and S. Smith, Science **265**, 1599 (1994).

[13] T. Odijk, Phys. Rev. E **77**, 060901(R) (2008).

[14] F. Brochard-Wyart, T. Tanaka, N. Borghi, and P.-G. de Gennes, Langmuir **21**, 4144 (2005).

[15] P. Cifra, J. Chem. Phys. **131**, 224903 (2009); P. Cifra, Z. Benková, and T. Bleha, J. Phys. Chem. B **113**, 1843 (2009).

[16] Y. Wang, D. R. Tree, and K. D. Dorfman, Macromolecules **44**, 6594 (2011).

[17] P. J. Hagerman and B. H. Zimm, Biopolymers **20**, 1481 (1981).

[18] J. Wang and H. Gao, J. Chem. Phys. **123**, 084906 (2005).

[19] For the persistence lengths of (5.3, 23, 53) nm, we obtained ($10^3$, $2 \times 10^2$, $10^3$) samples per simulation using (48, 48, 12) independent simulations, each with an equilibration of (2.07, 8.19, 20.6) $\times 10^8$ steps and production runs of (2.05, 2.05, 4.10) $\times 10^9$ steps.

[20] J. D. Chodera, W. C. Swope, J. W. Pitera, C. Seok, and K. A. Dill, J. Chem. Theory Comput. **3**, 26 (2007).

[21] Y. Yang, T. W. Burkhardt, and G. Gompper, Phys. Rev. E **76**, 011804 (2007); T. W. Burkhardt, Y. Yang, and G. Gompper, *ibid.* **82**, 041801 (2010).

[22] H. Yamakawa, *Modern Theory of Polymer Solutions*, edited by S. Rice (Harper and Row,

1971) pp. 269–285.

[23] R. B. Bird, C. F. Curtiss, and R. C. Armstrong, *Dynamics of Polymeric Liquids, Volume 2: Kinetic Theory* (Wiley, New York, 1987) pp. 298–299.

[24] B. H. Zimm, Macromolecules **13**, 592 (1980); J. G. de la Torre, A. Jimenez, and J. J. Freire, *ibid.* **15**, 148 (1982); D. Amorós, A. Ortega, and J. García de la Torre, *ibid.* **44**, 5788 (2011); M. L. Mansfield and J. F. Douglas, *ibid.* **41**, 5412 (2008).

[25] R. M. Robertson, S. Laib, and D. E. Smith, Proc. Natl. Acad. Sci. USA **103**, 7310 (2006); D. E. Smith, T. T. Perkins, and S. Chu, Macromolecules **29**, 1372 (1996); S. S. Sorlie and R. Pecora, *ibid.* **23**, 487 (1990).

[26] R. M. Jendrejack, D. C. Schwartz, M. D. Graham, and J. J. de Pablo, J. Chem. Phys. **119**, 1165 (2003).

[27] D. C. Morse, Macromolecules **31**, 7044 (1998).

[28] J. L. Harden and M. Doi, J. Phys. Chem. **96**, 4046 (1992).

[29] A. Balducci, P. Mao, J. Han, and P. S. Doyle, Macromolecules **39**, 6273 (2006); P. K. Lin, J. F. Chang, C. H. Wei, P. H. Tsao, W. S. Fann, and Y. L. Chen, Phys. Rev. E **84**, 031917 (2011).

[30] C. C. Hsieh, A. G. Balducci, and P. S. Doyle, Nano Lett. **8**, 1683 (2008).